Thermodynamics of Wax Precipitation in Petroleum Mixtures

C. Lira-Galeana and A. Firoozabadi
Reservoir Engineering Research Institute, Palo Alto, CA 94304

John M. Prausnitz
Chemical Engineering Dept., University of California, Berkeley
Chemical Sciences Div., Lawrence Berkeley Laboratory, Berkeley, CA 94720

A thermodynamic framework is developed for calculating wax precipitation in petroleum mixtures over a wide temperature range. The framework uses the experimentally supported assumption that precipitated wax consists of several solid phases; each solid phase is described as a pure component or pseudocomponent that does not mix with other solid phases. Liquid-phase properties are obtained from an equation of state. Calculated wax-precipitation data are in excellent agreement with experimental results for binary and multicomponent hydrocarbon mixtures, including petroleum.

Introduction

The broad volatility and melting-point range of hydrocarbon components found in petroleum causes formation of vapor, liquid, and solid phases in response to changes in pressure, temperature, or composition. When the temperature falls, heavy hydrocarbon components in the liquid and vapor may precipitate as wax crystals. In the petroleum industry, wax precipitation is undesirable because it may cause plugging of pipelines and process equipment. Wax precipitation is an old problem (Fagin, 1945; Goldman and Nathan, 1957; Ford et al., 1965) but only recently have attempts been made to develop a thermodynamic description.

Published methods for describing wax precipitation are often in poor agreement with experimental data; they tend to overestimate the amount of wax at temperatures below the cloud-point temperature, which is the temperature where wax first begins to precipitate. Computational tools based on regular-solution theory of mixtures as well as on equations of state (EOS) have been proposed to model wax precipitation (cf. Won, 1986, 1989; Hansen et al., 1988; K. S. Pedersen et al., 1991; Pedersen, 1993; Erickson et al., 1993). All of these methods assume that all the compounds that precipitate from the liquid or vapor form a *solid solution*. However, spectroscopic and calorimetric studies reported in the last few years by Snyder et al. (1992, 1993, 1994) and W. B. Pedersen et al. (1991) suggest that large hydrocarbons are mutually insoluble in the solid state.

To illustrate previous work, Figure 1 shows the essential thermodynamic equations for a three-phase flash calculation for a waxy crude oil mixture, assuming that only one solid phase is present; that phase is assumed to be a solid solution. At fixed temperature and pressure, a liquid phase (l) may coexist in equilibrium with a vapor phase (v) and a solid phase

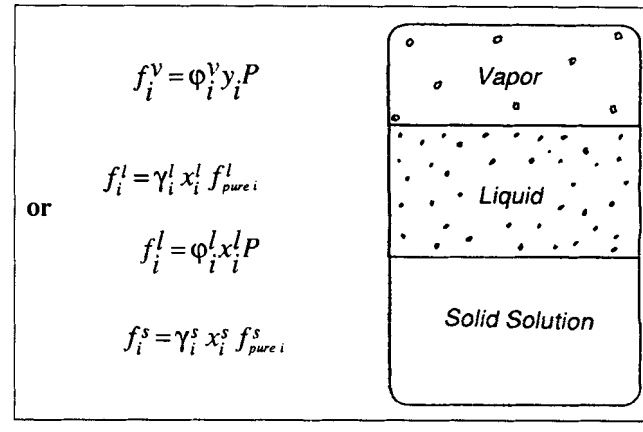

Figure 1. Typical vapor–liquid–solid-solution model for wax precipitation used by previous authors.

Correspondence concerning this article should be addressed to A. Firoozabadi.
Current address of C. Lira-Galeana: Instituto Mexicano del Petróleo, Eje Central L. Cárdenas 152, Col. San Bartolo Atepehuacán, C.P. 07730; Deleg. G. A. Madero, Mexico City, Mexico.

(s). At equilibrium, it is necessary that, for every component i

$$f_i^v = f_i^l = f_i^s, \qquad i = 1,2,\ldots,N, \tag{1}$$

where f is the fugacity and N is the number of components. An EOS can be used to describe the vapor phase. The liquid phase can either be described by an activity-coefficient model or by an EOS. The solid solution is often described by an activity-coefficient model (Prausnitz et al., 1986).

For vapor–liquid equilibria, it is common practice to use K factors, where $K_i^{vl} = y_i/x_i^l$; y_i is the mole fraction in the vapor phase and x_i^l is the mole fraction in the liquid phase. It can readily be shown that $K_i^{vl} = \varphi_i^l/\varphi_i^v$, where φ is the fugacity coefficient as found from an EOS.

For solid–liquid equilibria, there is an analogous K-factor: $K_i^{sl} = x_i^s/x_i^l$. It can readily be shown that

$$K_i^{sl} = \frac{\gamma_i^l}{\gamma_i^s}\left(\frac{f^l}{f^s}\right)_{\text{pure}\,i}, \tag{2}$$

where γ is the activity coefficient. At any temperature and pressure, the ratio $(f^l/f^s)_{\text{pure}\,i}$ can be calculated from the melting temperature, the melting enthalpy, and the heat capacities and densities of pure liquid i and pure solid i, as discussed elsewhere (Prausnitz et al., 1986). The effect of pressure is usually negligible, unless the pressure is very high and/or the temperature very low.

As suggested in Figure 1, there is an alternate method for calculating K_i^{sl}. If the fugacity coefficient (φ) in the liquid mixture is found from an EOS, while the solid phase is described by an activity coefficient model, then $K_i^{sl} = \varphi_i^l P/\gamma_i^s f_{\text{pure}\,i}^s$, where $f_{\text{pure}\,i}^s$ and φ_i^l are evaluated at the temperature and pressure of the mixture.

Won (1986) used two molecular thermodynamic models for describing the properties of the liquid phase. He used an EOS for computing φ_i^l for vapor–liquid equilibria and a modified regular-solution model to estimate the nonidealities of the liquid and solid solutions, γ_i^l and γ_i^s, respectively, for calculating liquid–solid equilibria. He neglected the effect of the heat-capacity difference of the solid and liquid, ΔCp_i on the ratio $(f^l/f^s)_{\text{pure}\,i}$.

In 1989, Won used his method to calculate the solubilities of n-C_{28} and n-C_{36} solids in n-C_5 and n-C_{12} at atmospheric pressure. He modified his earlier model by (1) incorporating an extended regular-solution expression for activity coefficients in the liquid phase; (2) assuming a pure-solid phase for the heavier hydrocarbon component; and (3) including the heat-capacity effect on the ratio $(f^l/f^s)_{\text{pure}\,i}$. The heat-capacity contribution improved prediction of the solubilities of the heavier n-alkanes in the liquid phase.

In 1988 Hansen et al. observed that Won's model (1986) was not satisfactory for calculation of the cloud-point temperatures of 17 oil mixtures. They reasoned that since Won's model gives activity coefficients close to unity for the wax-forming components, the K_i^{sl}-factor of Eq. 2 essentially depends only on the ratio of $f_{\text{pure}\,i}^l$ to $f_{\text{pure}\,i}^s$. These authors proposed to use the polymer-solution theory of Flory (1953) for describing nonidealities in the liquid phase, and assumed $\gamma_i^s = 1$. Three adjustable parameters in the proposed model were estimated from measured cloud-point data. Using parameters from these data, agreement between calculated and experimental cloud points was good.

Extensive data on cloud-point temperature and amount-of-wax deposition became available in 1991. K. S. Pedersen et al. (1991) evaluated the performance of Won's (1986) and Hansen et al.'s (1988) procedures with the data; these models significantly overestimated the amount of wax deposition and cloud-point temperature. To obtain an improved representation, K. S. Pedersen et al. (1991) proposed to modify Won's model by (1) using solubility parameters δ_i^l and δ_i^s with one adjustable parameter for each of the solid and liquid phases; (2) incorporating the paraffinic/naphthenic/aromatic (PNA) split for each pseudocomponent of the C_{7+}-fraction; (3) modifying the melting-enthalpies of the P-, N- and A-pseudocomponents by means of one adjustable parameter; and (4) incorporating the effect of the heat-capacity difference, ΔCp_i on the computation of $(f^l/f^s)_{\text{pure}\,i}$ with two-adjustable parameters. The five regression parameters were obtained by matching data and model results. This procedure revealed that (1) the solid solution is highly nonideal; and (2) the heat capacities strongly influence the solid deposition. While this model provided an improved representation of wax precipitation over previous procedures, it requires abundant experimental data for determining various model parameters.

To overcome the overestimation of wax deposition by available models, Pedersen (1993) recently suggested assigning high fugacity coefficients to selected components (pseudocomponents) of the crude oil. Based on an empirical relationship with constants estimated from experimental deposition data, Pedersen proposed that only a portion of the heptanes-plus fraction of an oil may coexist in solid–liquid equilibrium. Pedersen used the SRK-EOS (Soave, 1972) to describe gas and liquid phases and assumed the wax to be an ideal solid solution. Figure 2 illustrates the performance of Pedersen's latest model for two oil mixtures (the compositions are in Table 1).

In this article, we present a thermodynamic method for wax precipitation with the assumption that wax deposition is a multisolid-phase process. Each solid phase is a pure component (or pseudocomponent); its existence or nonexistence is determined by phase-stability considerations. An EOS is used to describe properties of the gas and of the liquid. Calculated results are compared with experimental deposition data for binary model systems and for petroleum mixtures.

Multisolid-Phase Model

Recent reports in the literature describe the physics of solidification of crude-oil constituents below the cloud-point temperature. Solid-phase transitions and spontaneous demixing are parts of the wax-precipitation process. Differential-scanning-calorimetry studies by W. B. Pedersen et al. (1991) on a number of North Sea crude oils show phase transitions below the cloud-point temperature of various petroleum mixtures. Similarly, spectroscopic studies of Snyder et al. (1992, 1993, 1994) on the kinetics of microphase demixing of binary hydrocarbon mixtures show that the phase behavior below the cloud-point temperature of these systems follows an ini-

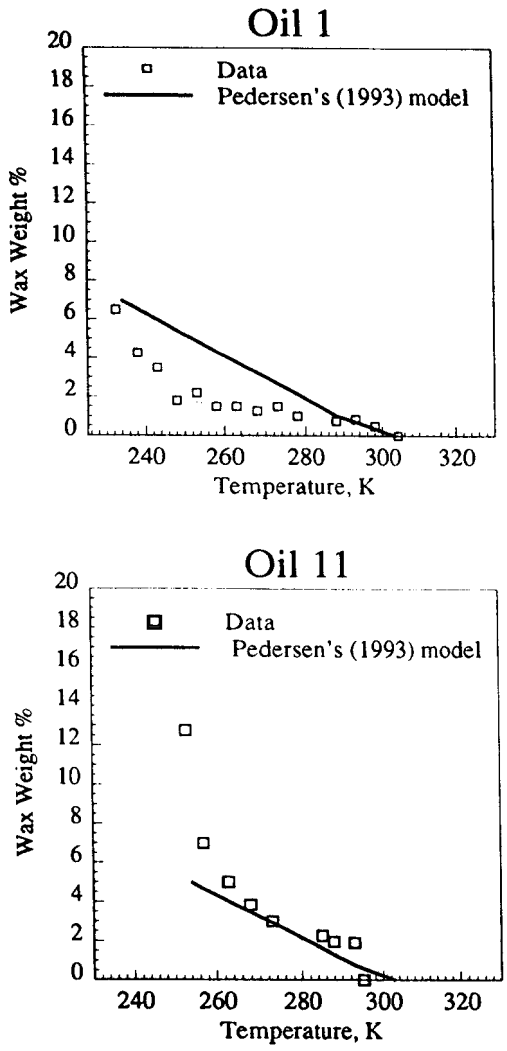

Figure 2. Measured vs. calculated wax-precipitation results for two petroleum mixtures at 1 bar.

tial (unstable) solid–solution state where the components are temporarily miscible in all proportions. After a characteristic time, however, spontaneous demixing of the solid solution leads to the final stable state. Snyder et al. found that the final stable phases consist predominantly of *pure components*.

These independent experimental studies suggest that wax precipitation in multicomponent oil systems produces a solid mass that contains *mutually immiscible* precipitating components. Since the solubility of each precipitating species is a strong function of the temperature, it is expected that, as cooling proceeds, only a selected number of precipitating components will coexist in solid–liquid equilibrium. On the contrary, by assuming that *all* the crude oil components can coexist in the solid state, the *solid–solution* model of Figure 1 overestimates the amount of precipitated wax. A more realistic thermodynamic procedure for calculating wax precipitation should be based on the following: (a) the precipitated species from the crude oil consist essentially of pure-(pseudo) components that *do not mix* with other solid phases after precipitation; and (b) the number and identity of (pseudo) components that precipitate as pure solids are determined through phase-stability analysis.

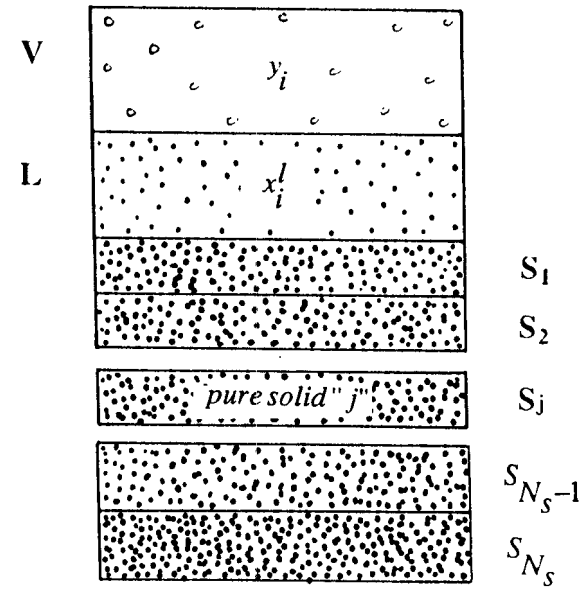

Figure 3. Proposed multisolid-phase model for wax precipitation.

Figure 3 shows a schematic separation vessel for a petroleum mixture that flashes into a vapor, a liquid, and *several* immiscible solid phases of pure components. The multisolid-phase model shown in Figure 3 is best illustrated by a plot of wax precipitated vs. temperature, shown in Figure 4. Below the cloud-point temperature, the precipitation of wax constitutes a consecutive deposition process that precipitates several pure solids, each completely *immiscible* with the others in the solid state. At a given temperature, the total amount of precipitated wax is the sum of the contributions of all solid phases that exist in equilibrium with the liquid at that temperature.

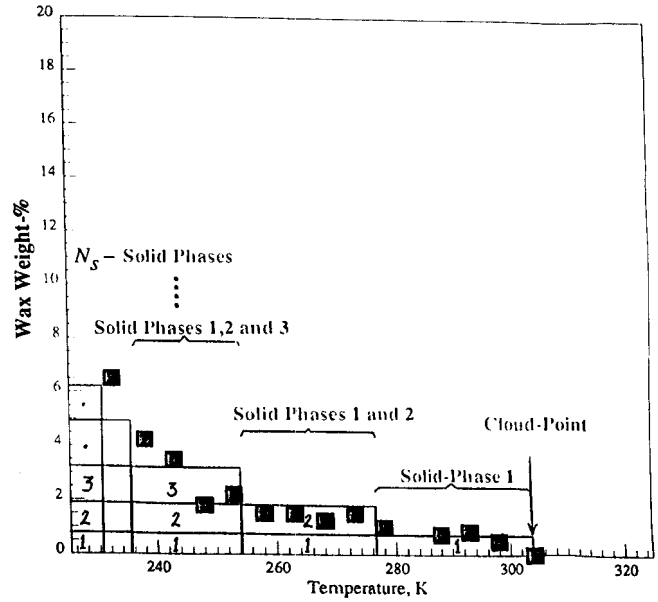

Figure 4. Multisolid-phase precipitation concept for a petroleum mixture below its cloud-point temperature.

From stability considerations, it follows that (pseudo) component i may exist as a pure solid if

$$f_i(P,T,z) - f^s_{\text{pure}\,i}(P,T) \geq 0, \qquad (i=1,2,\ldots,N), \quad (3)$$

where $f_i(P, T, z)$ is the fugacity of component i with feed composition z. This stability criterion is easily derived from Eq. 5 of Michelsen (1982). The mixture components that fulfill the preceding expression will precipitate, while those that do not will only be present in the liquid and vapor states. The Peng–Robinson EOS (Peng and Robinson, 1976) in the form described by Robinson et al. (1985) is used for calculating fugacities for components in the fluid phases.

EOS Modeling

At fixed temperature and pressure, for every component i, the multisolid–phase model must satisfy

$$f_i^v = f_i^l = f^s_{\text{pure}\,i} \qquad (i = N-(N_s-1),\ldots,N) \quad (4)$$

$$f_i^v = f_i^l \qquad (i=1,2,\ldots,N-N_s), \quad (5)$$

where N_s is the number of solid phases determined from Eq. 3. Coupling material balances with Eqs. 4 and 5, there will be a set of N_s+2N-1 simultaneous equations with N_s+2N-1 unknowns (see the Appendix). If no vapor phase is present, the model reduces to N_s+N-1 variables. This multiphase-flash problem can be solved by Newton's method.

As required for Eqs. 4 and 5, the fugacities in the vapor and liquid phases are evaluated through the EOS. The solid-phase fugacities of the pure components, $f^s_{\text{pure},i}$ can be evaluated from the ratio $(f^s/f^l)_{\text{pure}\,i}$. Neglecting the effect of pressure, this ratio is obtained from pure-component data for component i as shown elsewhere (Prausnitz et al., 1986):

$$\ln\left(\frac{f^s}{f^l}\right)_{\text{pure}\,i} = -\frac{\Delta h_i^f}{RT}\left(1-\frac{T}{T_i^f}\right) + \frac{1}{R}\int_T^{T_i^f}\frac{\Delta Cp_i}{T}\,dT - \frac{1}{R}\int_T^{T_i^f}\Delta Cp_i\,dT, \quad (6)$$

where superscript f refers to fusion. The liquid-phase fugacity is obtained from $f^l_{\text{pure}\,i} = \varphi^l_{\text{pure}\,i}(P,T)P$, where the fugacity coefficient, $\varphi^l_{\text{pure}\,i}$ is obtained from the EOS. In Eq. 6, T_i^f is the fusion (melting) temperature; Δh_i^f is the enthalpy of fusion; and $\Delta Cp_i = Cp_i^l - Cp_i^s$, where Cp_i is the heat capacity of pure i at constant pressure. For hydrocarbons and petroleum mixtures, a simple cubic EOS such as the PR-EOS describes the liquid and gas phases well (away from the gas–liquid critical region, cf. Firoozabadi, 1988).

The flash calculation proceeds as follows:

(a) Characterize the *plus* fraction of a given petroleum mixture using, say 7 to 12 pseudocomponents. Assign critical properties and acentric factors to all the pseudocomponents using available correlations. In this work, we used the correlations proposed by Cavett (1964), but other similar methods (Twu, 1984; Riazi and Daubert, 1980) may be used.

(b) For hydrocarbon pairs, use the component critical volumes, v_{c_i} to compute the values of binary interaction parameters for the EOS, k_{ij}^{EOS}, from the correlation of Chueh and Prausnitz (1967):

$$k_{ij}^{EOS} = 1 - \left[\frac{2v_{c_i}^{1/6}v_{c_j}^{1/6}}{v_{c_i}^{1/3}+v_{c_j}^{1/3}}\right]. \quad (7)$$

Equation 7 is used to find the cross-parameter a_{ij} in the EOS: $a_{ij} = (a_i a_j)^{1/2}\,[1-k_{ij}^{EOS}]$. The critical volumes in Eq. 7 are estimated from the expression $v_{ci} = (RT_{ci}/P_{ci})\,(0.290 - 0.085\omega_i)$, where ω_i is the component acentric factor, as estimated from Edmister acentric factor formula (Edmister, 1958).

(c) Perform stability analysis (Eq. 3) for the feed at system temperature and pressure. Stability analysis gives the number and identities of the precipitating pure components (pseudo-components) that form solid phases.

(d) Solve the system of equations described in the Appendix. For liquid–multisolid equilibria, the unknowns are N_s solid-to-feed molar fractions, S_j/F, and $(N-1)$ compositions in the liquid phase, x_i^l. For vapor–liquid–multisolid systems, the unknowns are $2(N-1)$ compositions for the vapor and liquid phases, y_i, x_i^l, respectively, N_s solid-to-feed molar phase fractions, (S_j/F), and the fraction of feed that exists as vapor, (V/F).

Correlations for Calculating Fugacities of Pure Solids

As shown by Eq. 6, the fugacity of solid-component i depends upon the melting properties of component i: the melting-point temperature, T_i^f, the enthalpy of fusion, Δh_i^f, and the heat-capacity difference, ΔCp_i. In previous work, these quantities have been evaluated using different procedures. Unless stated otherwise, in this article the melting-point properties of the components were evaluated as follows.

Melting-point temperature, T_i^f

Won (1986) has given a correlation for the melting points of pure n-alkanes:

$$T_i^f = 374.5 + 0.02617I_i - 20172/I_i, \quad (8)$$

where T is in degrees kelvin and I_i is molecular weight in grams per mole. To replace Eq. 8, we used experimental melting-point data of normal paraffinic (C_6–C_{30}), naphthenic (C_6–C_{30} alkylcycloalkanes), and aromatic (C_6–C_{30} alkylbenzenes) hydrocarbons (Research Project 44, API, 1964) to derive the following correlation (temperature in K)

$$T_i^f = 333.46 - 419.01\exp(-0.008546I_i). \quad (9)$$

In the preceding equation, as the molecular weight increases, the calculated melting points of petroleum fractions gradually lose the paraffinic contribution. The asymptotic temperature relation of Eq. 9 corresponds to the average melting temperature of heavy naphthenic and aromatic hydrocarbons with carbon numbers above 30. Figure 5 shows Eq. 9 along with experimental data.

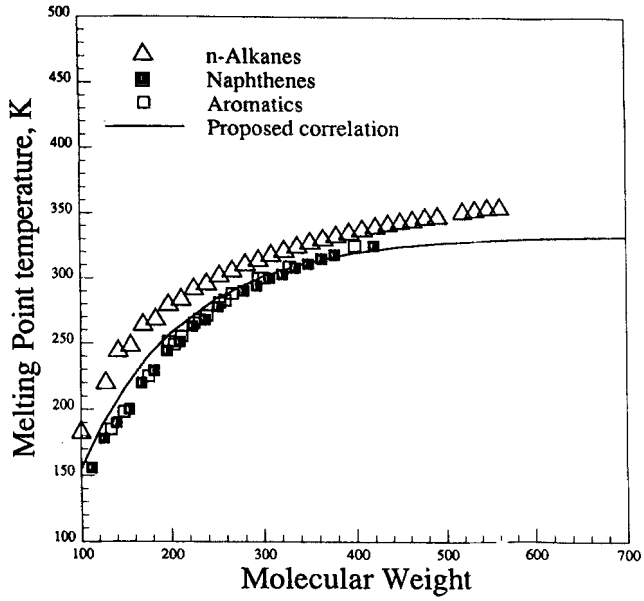

Figure 5. Melting-point temperatures of hydrocarbons.

Enthalpy of fusion, Δh_i^f

Won (1986) developed a correlation for calculating the melting-point enthalpies of paraffinic hydrocarbons using the molecular weight of the paraffins as a characterization variable. The correlation has the form,

$$\Delta h_i^f = 0.1426 I_i T_i^f. \tag{10}$$

The constant (0.1426), represents the average slope when the entropy of fusion, $(\Delta h_i^f/T_i^f)$ is plotted against the molecular weight of paraffinic hydrocarbons. K. S. Pedersen et al. (1991) argued that the melting enthalpies of different hydrocarbon species found in a petroleum fluid have a broad range of values for the same molecular weight, and therefore Eq. 10 overestimates the wax amount below the cloud-point temperature. These authors concluded that Eq. 10 should not be applied to petroleum mixtures.

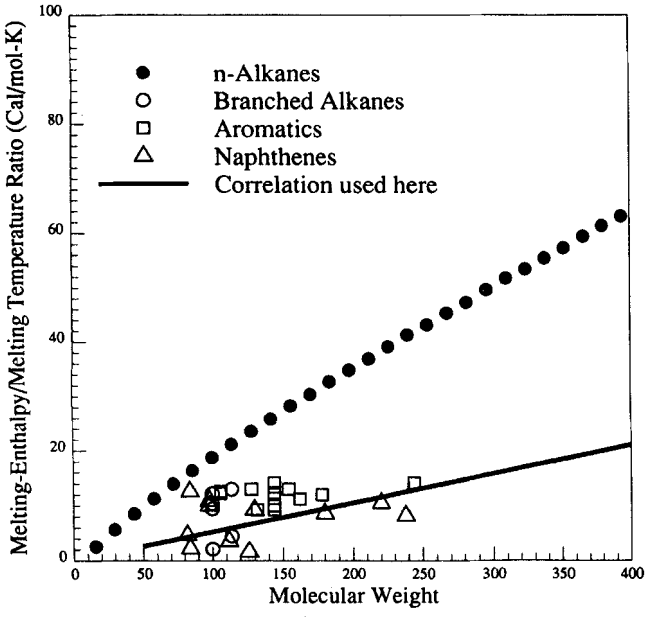

Figure 6. Entropies of fusion of hydrocarbons.

Figure 6 shows experimental data (Research Project 44, API, 1964) for the entropy of fusion of various P-, N- and A-hydrocarbons as a function of molecular weight. The melting entropies of n-paraffins are indeed higher than those of N- and A-hydrocarbons with the same molecular weight. However, when the slope of the entropy-of-fusion vs. molecular-weight line for normal paraffins given by Eq. 10 is decreased by a factor between 2 and 3, the resulting entropies tend to deviate from purely paraffinic behavior to a more "multiensemble" hydrocarbon environment, which may correspond more closely to the wax-precipitation context. Since the presence of paraffinic components decreases as the carbon number increases, smaller enthalpies of fusion than those proposed by Eq. 10 may be more representative for wax precipitation. A similar reduction process of the enthalpies of hydrocarbons was used by K. S. Pedersen et al. (1991) and by Erickson et al. (1993). We suggest the following expression for the enthalpy of fusion:

$$\Delta h_i^f = 0.05276 I_i T_i^f, \tag{11}$$

where Δh_i^f is in calories/mole.

Heat capacity of fusion ΔCp_i

Toward including the heat-capacity data, K. S. Pedersen et al. (1991) analyzed the trend of the experimental heat-capacity data with molecular weight for various n-alkanes and found that the data could be represented by the expression

$$\Delta Cp_i = \alpha I_i + \beta I_i T, \tag{12}$$

where ΔCp_i is in calories/mole-K. Correlation coefficients α (0.3033 cal/g·K) and β (-4.635×10^{-4} cal/g·K^2) were determined by K. S. Pedersen et al. by tuning their model with experimental precipitation data for 17 North Sea crude oils.

Here, we correlate heat-capacity data of heavy n-alkanes (Finke et al., 1954; Spaght et al., 1932) with molecular weight and temperature using the function given by Eq. 12. For the liquid phase below the melting point temperature, the heat capacity is assigned the value at the melting point. For the solid phase above the melting point temperature, the heat capacity at the melting point is assigned. By using this procedure, we found that the values of the correlation coefficients α and β in Eq. 12 are close to those found by K. S. Pedersen et al. (1991). Therefore, we use their correlation coefficients. We also assume that hydrocarbon species other than n-alkanes follow Eq. 12 with the same coefficients. To test the validity of this assumption, thermal data of selected high-molecular-weight hydrocarbons other than n-alkanes (Parks et al., 1949; Fischl et al., 1945) were compared with predictions from Eq. 12. The predicted heat-capacity differences were 10 to 20% higher than the heat capacity data of heavy naphthenic and aromatic hydrocarbons. Therefore, the heat capacity correlation given by Eq. 12 appears to provide a reasonable estimate for the thermal effects on the fugacities of solid-forming components in petroleum mixtures.

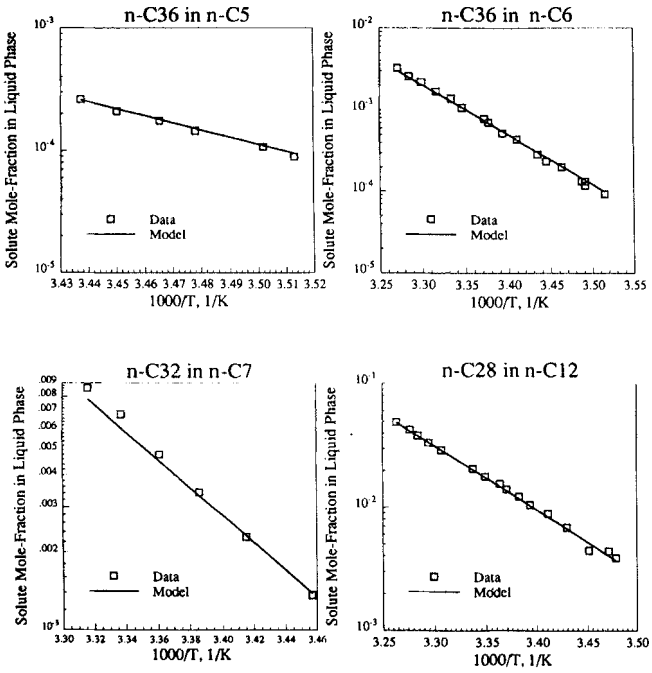

Figure 7. Measured and predicted solid solubilities for four binary alkane mixtures at 1 bar.

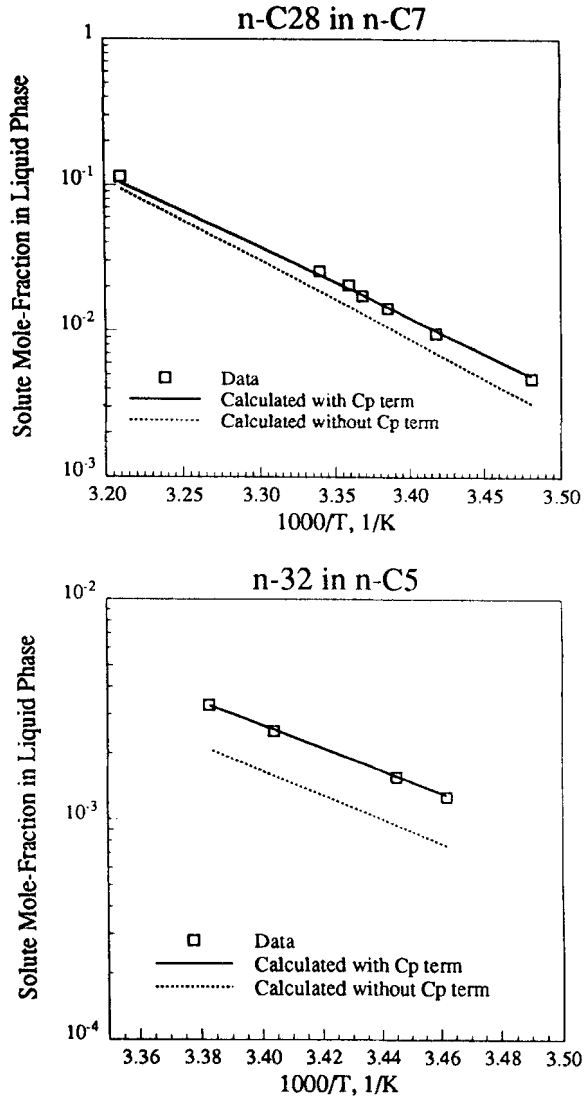

Figure 8. Effect of heat-capacity difference ΔCp on calculated solid solubilities for two alkane mixtures at 1 bar.

Results

Binary systems

Madsen and Boistelle (1976, 1979) measured binary solid solubilities of six n-alkane mixtures (n-C_{32} in n-C_5 and n-C_7; n-C_{28} in n-C_7 and n-C_{12}; and n-C_{36} in n-C_5 and n-C_6). For normal paraffins, we used the n-alkane-based correlations for estimating the melting-point temperature and enthalpy of fusion given by Won (Eqs. 8 and 10). Figures 7 and 8 show calculated and experimental results. Figure 7 shows that the calculated solubilities are predicted very well for all systems. The effect of the heat-capacity data on calculated results is illustrated in Figure 8 for systems n-C_{28}–n-C_7 and n-C_{32}–n-C_5. Including the ΔCp_i term provides a significant improvement. A similar effect was observed for other binary systems. The results shown in Figures 7 and 8 are predicted without any parameter adjustment.

Crude-oil systems

Table 1 shows compositions, component molecular weights, and plus-fraction-specific gravities of eight petroleum mixtures. W. B. Pedersen et al. (1991) have provided extensive data on wax-formation behavior of these crude oils. The mixture numbers are the same as those used by these authors.

The types of crude oils shown in Table 1 cover a variety of oil mixtures. Mixtures 10, 12 and 15 originate from light petroleum systems of the gas-condensate type. Mixtures 8 and 11 originate from heavy oils. For calculation purposes, the *plus* fractions in all mixtures require a systematic characterization procedure. For each oil, we used the experimental molecular weight, mole fraction, and specific-gravity data of the *plus* fraction to generate a number of pseudocomponents that preserve the measured characterization properties of the heavy fraction. The carbon-number distribution of petroleum waxes has been studied by some investigators. Ronningsen et al. (1991) reported wax composition of a given crude from carbon number C_{16} to much higher carbon numbers. They estimated C_{40+} content of a particular wax to be around 50% (volume). They also cautioned that the wax that they analyzed inevitably contained some trapped oil that affects the lower carbon number. In 1994, Bishop and Philp, using a high-temperature gas chromatographic technique, have shown that the spectrum of hydrocarbon components found in petroleum waxes begins at approximately C_{20-25} but, unlike Ronningsen et al. (1991), Bishop and Philp analyzed the fraction of hydrocarbon components beyond C_{40+} and found that the carbon-number distribution extends to C_{90-100}. From these two studies, it is evident that for precipitation calculations, a pseudocomponent slate with components whose molecular weights exceed 1,000 is desirable. The two-parameter gamma distribution function (Johnson and Kotz, 1970; Whitson, 1983) was used for generating the molar distributions for the plus fractions of each of the eight petroleum

Table 1. Compositions and Properties of Oil Mixtures

Oil No.	1		2		5		8		10		11		12		15	
Comp.	Mol %	Mol wt.	Mol %	Mol wt.	Mol %	Mol wt.	Mol %	Mol wt.	Mol %	Mol wt.	Mol %	Mol wt.	Mol %	Mol wt.	Mol %	Mol wt.
C_1	1.139				0.056				0.016						0.021	
C_2	0.507		0.009		0.368		0.113		0.145		0.100		0.173		0.254	
C_3	0.481		0.476		1.171		1.224		1.392		0.118		1.605		1.236	
i-C_4	0.563		0.585		0.466		0.645		1.180		0.106		1.148		0.588	
C_4	0.634		1.572		1.486		2.832		3.088		0.099		3.596		2.512	
i-C_5	1.113		1.705		0.961		1.959		2.980		0.162		3.086		1.955	
C_5	0.515		1.985		1.396		3.335		3.802		0.038		4.171		3.485	
C_6	2.003		1.491		2.251		5.633		7.207		0.458		7.841		6.842	
C_7	5.478	90.9	9.110	92.3	6.536	88.8	9.933	92.8	11.333	94.1	2.194	90.8	11.11	94.1	12.85	92.2
C_8	8.756	105.0	10.84	105.9	8.607	101.0	10.75	106.3	12.465	107.0	2.847	106.5	13.43	105.4	13.98	105.4
C_9	7.222	117.7	7.413	120.0	4.882	116.0	7.179	120.0	7.784	122.0	1.932	122.3	9.419	119.0	9.190	119.0
C_{10}	5.414	132.0	6.394	133.0	2.830	133.0	6.561	134.0	5.314	136.0	5.750	135.0	5.583	135.0	6.435	134.0
C_{11}	5.323	148.0	5.649	148.0	3.019	143.0	5.494	148.0	5.033	147.0	4.874	149.0	4.890	148.0	5.118	148.0
C_{12}	4.571	159.0	5.270	163.0	3.119	154.0	4.547	161.0	3.989	161.0	5.660	162.0	3.864	162.0	4.111	161.0
C_{13}	5.289	172.0	4.541	177.0	3.687	167.0	4.837	175.0	3.869	175.0	6.607	176.0	4.298	175.0	4.231	175.0
C_{14}	4.720	185.0	4.921	190.0	3.687	181.0	3.700	189.0	3.627	189.0	6.149	189.0	3.272	188.0	3.682	188.0
C_{15}	4.445	197.0	3.903	204.0	3.637	195.0	3.520	203.0	3.165	203.0	5.551	202.0	2.274	203.0	3.044	202.0
C_{16}	3.559	209.0	2.894	217.0	3.079	207.0	2.922	216.0	2.311	214.0	5.321	213.0	2.791	216.0	2.255	214.0
C_{17}	3.642	227.0	3.420	235.0	3.657	225.0	3.072	233.0	2.472	230.0	5.022	230.0	2.311	232.0	2.405	230.0
C_{18}	3.104	243.0	2.399	248.0	3.289	242.0	2.214	248.0	2.815	244.0	4.016	244.0	1.960	246.0	2.006	245.0
C_{19}	2.717	254.0	2.737	260.0	3.109	253.0	2.493	260.0	2.110	258.0	4.176	256.0	1.821	256.0	1.766	257.0
C_{20}*	2.597	262.0	0.909	269.0	38.4+	423.0	17.0+	544.0	14.4+	418.0	38.8+	473.0	11.3+	388.0	12.0+	399.0
C_{21}	1.936	281.0	2.207	283.0												
C_{22}	2.039	293.0	1.463	298.0												
C_{23}	1.661	307.0	1.226	310.0												
C_{24}	1.616	320.0	0.933	322.0												
C_{25}	1.421	333.0	1.327	332.0												
C_{26}	1.233	346.0	1.074	351.0												
C_{27}	1.426	361.0	0.852	371.0												
C_{28}	1.343	374.0	0.900	382.0												
C_{29}	1.300	381.0	0.662	394.0												
$C_{30}+$	13.23	624.0	8.177	612.0												
Sp.Gr.$_+$	0.953		0.935		0.893		0.934		0.880		0.963		0.872		0.887	

*C_{20} or C_{20+}.

mixtures of Table 1. Figure 9 shows the shape of the molar distributions for all mixtures, and Table 2 shows the distribution-function parameters for each fraction. Table 3 shows the resulting characterization parameters for the heptanes-plus fraction of Oil 1.

Figures 10 and 11 show results using our multisolid-phase model. These figures indicate that the multisolid-phase assumption appears to represent the wax-formation process in real petroleum mixtures. For all mixtures, the predicted trend for the solid amount with temperature is in good agreement with experiment. At a given temperature, the wax weight percent that precipitates from crude oil is calculated for 1 mol of feed from the relation

$$\text{Wax weight } \% = \frac{\text{total precipitated mass}}{\text{mass of feed oil}} \times 100 = \frac{\sum_j^{N_s} I_j \left(\frac{S_j}{F}\right)}{\sum_i^{N} z_i I_i} \times 100.$$

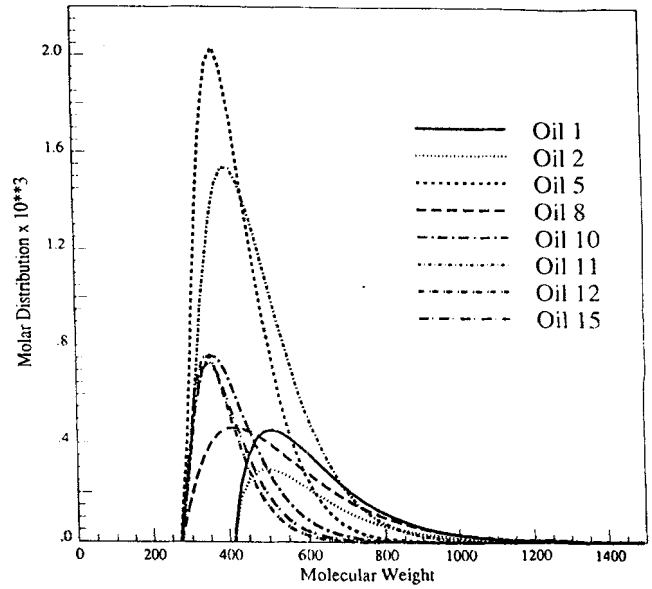

Figure 9. Estimated molar distribution for *plus* fractions of oil mixtures.

Table 2. Statistical Properties for Molar Distributions of Oil Mixtures

Oil No.	Initial mol wt.	Mean	Variance
1	413.0	624.0	24,194.5
2	413.0	612.0	23,020.7
5	273.0	423.0	8,006.8
8	273.0	544.0	34,802.9
10	273.0	418.0	8,442.9
11	273.0	473.0	14,282.2
12	273.0	388.0	5,105.8
15	273.0	399.0	6,300.0

Predictions for Oils 10, 12 and 15, which originate from gas-condensate mixtures, are as good as those for Oils 8 and 11, which originate from heavy-petroleum systems.

Equation 3 provides a useful criterion for determining those components that precipitate. Application of the stability test for all the mixtures revealed that, for temperatures in excess of 230 K, hydrocarbon components with molecular weights less than, say 400, are unlikely to participate in the solid wax. For Oil 1, up to four different solid phases characterize the predicted wax weight percent along the indicated temperature range. These four solids consist of pseudocomponents with average molecular weights 750, 800, 950 and 1350, respectively (Table 3). Similar molecular weights characterize the solid phases for the other systems. The model proposed in this study suggests that, in typical real systems, the "carrying" capacity of the light fraction of the oil keeps hydrocarbons with molecular weights ranging from 100 (C_7) to around 400 (C_{25}) dissolved in the liquid phase (oil), in agreement with the wax analysis by Bishop and Philp (1994). The solid-solution models predict the presence of light hydrocarbons in the solid wax (Won, 1989).

Figure 12 shows the solid-phase-appearance history of Oil 1. As cooling proceeds, the multisolid-phase model predicts the appearance of solid phases along the experimental temperature range in a consecutive manner, as illustrated in Figure 4. From our experience, the more discontinuous the experimental precipitation curve of a particular oil (as occurs for Oils 2 and 15), the larger the number of precipitated

Table 3. EOS-Characterization for the Heptanes-Plus Fraction of Oil 1

No.	mol %	mol. wt.	Tc/K	Pc/bar	ω	Vc/cm^3/mol
1	5.417	91.00	521.40	32.49	0.340	349.00
2	8.658	104.95	550.30	29.98	0.417	388.80
3	7.140	117.05	572.80	28.25	0.478	421.60
4	20.364	152.35	630.28	23.87	0.633	517.96
5	9.062	190.79	680.00	20.29	0.779	626.15
6	10.18	225.70	716.55	17.61	0.901	725.98
7	9.158	269.99	754.20	14.92	1.051	847.40
8	7.274	332.08	795.87	12.29	1.258	897.90
9	5.260	407.07	835.30	10.40	1.507	1,087.6
10	4.638	529.05	888.40	8.92	1.848	1,107.3
11	2.170	649.95	935.20	8.58	2.038	1,152.0
12	1.169	750.04	970.80	8.50	2.160	1,143.5
13	1.407	799.45	987.30	7.52	2.129	1,297.60
14	0.703	949.47	1,032.15	6.49	2.190	1,450.00
15	0.350	1,350.09	1,173.7	5.35	2.248	2,021.49

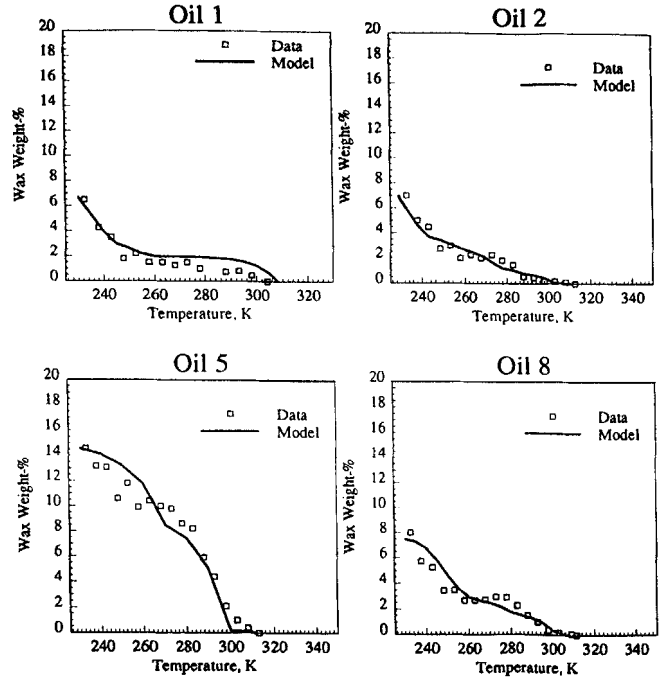

Figure 10. Experimental and predicted wax-precipitation results for Oils 1, 2, 5 and 8.

phases predicted by the model (8 and 12 solid phases, respectively). On the other hand, for fluid systems showing an abrupt jump in the experimental precipitation-vs.-temperature curve (Oils 5 and 11), a small number of precipitated solid phases provides a good representation of the data. The characterization technique employed here for wax calculations differs from the conventional characterization schemes for hydrocar-

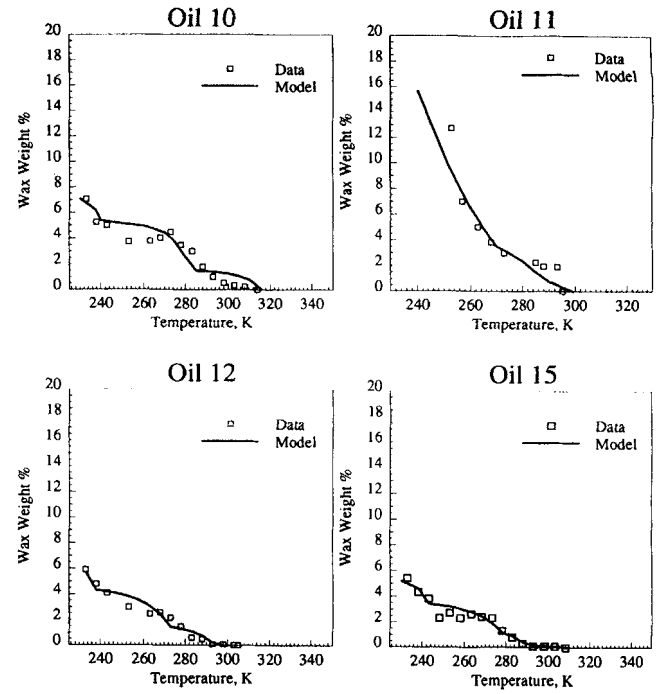

Figure 11. Experimental and predicted wax-precipitation results for Oils 10, 11, 12 and 15.

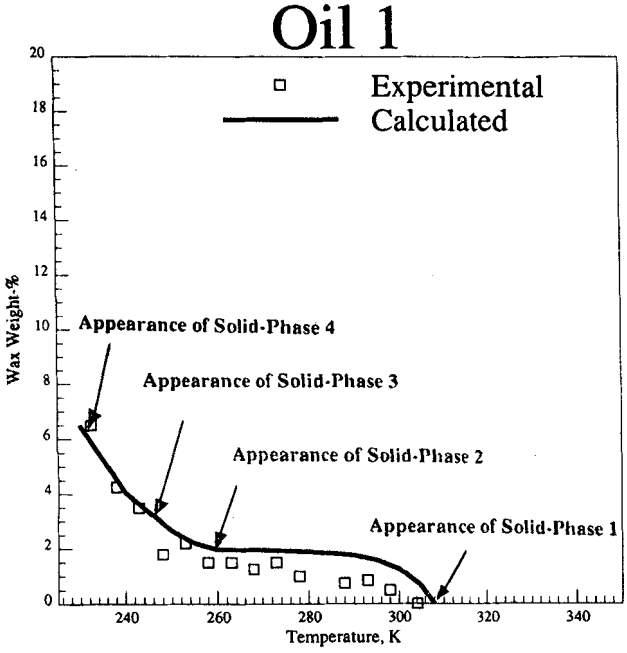

Figure 12. Predicted solid-phase-appearance temperatures for Oil 1 as cooling proceeds.

bons where the number of pseudocomponents could be regarded as a model parameter. There is an optimum number of pseudocomponents that will yield the best representation of the experimental data. Our approach contrasts with other characterization schemes in the sense that increasing the number of pseudocomponents is *only* expected to improve the accuracy of the representation.

Table 4 shows a comparison between experimental and calculated cloud-point temperatures for all mixtures considered here. From the equations given in the Appendix, the cloud-point temperature of a given petroleum mixture is that temperature where the molar ratio of the first precipitating component of the system (S_1/F) is greater than zero but smaller than a small positive value (10^{-8}). The calculated cloud-point temperatures compare well with the data for all mixtures. We did not adjust any parameter in the calculation of wax precipitation. Unlike other methods, the method discussed here reproduces the experimentally observed discontinuous deposition behavior of real petroleum systems.

Conclusions

An EOS-based molecular thermodynamic method for calculating wax precipitation in petroleum mixtures has been tested with experimental data. The method is based on the experimentally supported assumption that wax precipitation is a multisolid-phase precipitation process. The number and identity of the potential precipitated phases can be determined by a simple stability test. Application of this method to several petroleum mixtures suggests that the precipitated waxy material consists of high-molecular-weight hydrocarbons with average carbon-atom numbers above 25. Calculated results of the new method reproduce experimental liquid-wax equilibria for several oil mixtures, indicating that the proposed method is both simple and accurate, requiring no adjustable mixture parameters.

Table 4. Experimental and Calculated Cloud-Point Temperatures

Oil No.	Exp. K	Calc. K	Exp.-Calc. K
1	304.15	305.9	−1.75
2	312.15	311.8	0.35
5	313.15	312.4	0.75
8	311.15	308.2	2.95
10	314.15	316.0	−1.85
11	295.15	299.3	−4.15
12	305.15	301.2	3.95
15	308.15	309.5	−1.35

Acknowledgments

This work was supported by the Director, Office of Energy Research, Office of Basic Energy Sciences, Chemical Sciences Division of the U.S. Department of Energy, under Contract DE-AC03-76SF00098. C. L.-G. acknowledges CONACYT; DEPFQ-UNAM and the Mexican Institute of Petroleum (IMP), Mexico City, Mexico, for a fellowship. Additional support from Norsk Hydro, A/S, Saudi Aramco, and Texaco, Inc., is greatly appreciated. Dr. Andrzej Anderko of Simulation Sciences, Inc., Brea, CA, provided generous help and discussion during the early stages of this work

Notation

K = partition coefficient
L = moles of liquid phase
P = pressure
R = gas constant
S = moles of solid phase
v = molar volume
x = solid composition, depending on superscript
z = overall (feed) mole fraction
x, y, z = composition vectors
ρ = density
Σ = sum operator

Subscript

c = property at the critical point

Literature Cited

American Petroleum Institute, *Selected Values for Physical and Thermodynamic Properties of Hydrocarbons and Related Compounds*, Res. Proj. 44, Texas A&M Univ., College Station, sec. *m* (1964).

Bishop, A., and P. Philp, "Prediction of Potential Wax Deposition Problems During Petroleum Production," Internal Rep., Organic Geochemistry Group, Univ. of Oklahoma, Norman (1994).

Cavett, R. H., "Physical Data for Distillation Calculations, Vapor-Liquid Equilibria," *Proc. API Div. of Refining Meeting*, San Francisco (May 15, 1964).

Chueh, P. L., and J. M. Prausnitz, "Vapor-Liquid Equilibria at High Pressures: Calculation of Partial Molar Volume in Non-Polar Liquid Mixtures," *AIChE J.*, **13**(6), 1099 (1967).

Edmister, W. C., "Compressibility Factors and Equations of State," *Pet. Refiner*, **37**(4), 173 (1958).

Erickson, D. D., V. G. Niesen, and T. S. Brown, "Thermodynamic Measurement and Prediction of Paraffin Precipitation in Crude Oil," paper SPE 26604, Tech. Conf. and Exhibit of the Soc. of Pet. Engrs., Houston (Oct. 3–6, 1993).

Fagin, K. M., "Automatic Scrapers Used in West Edmond Oil Wells," *Pet. Eng.*, 105 (June, 1945).

Finke, H. L., M. E. Gross, G. Waddington, and H. M. Huffman, "Low-Temperature Thermal Data for the Nine Normal Paraffin Hydrocarbons from Octane to Hexadecane," *J. Amer. Chem. Soc.*, **76**, 333 (1954).

Firoozabadi, A., "Reservoir-Fluid Phase Behavior and Volumetric Prediction with Equations of State," *J. Pet. Tech.*, 397 (Apr., 1988).

Fischl, F. B., B. F. Naylor, C. W. Ziemer, G. S. Parks, and J. G. Aston, "The Heat Capacity, Heat of Fusion and Entropy of 11-*n*-decylheneicosane," *J. Phys. Chem.*, **67**, 2075 (1945).
Flory, P. J., *Principles of Polymer Chemistry*, Cornell Univ. Press, Ithaca, NY (1953).
Ford, P. E., J. W. Ells, and R. J. Russell, "Frequent Pigging Helps Move Waxy Crude Below Its Pour-Point," *Oil & Gas J.*, 183 (May, 1965).
Goldman, M. S., and C. C. Nathan, "Prevention of Paraffin Deposition and Plugging," U.S. Patent No. 2,817,635 (Dec. 24, 1957).
Hansen, J. H., Aa. Fredenslund, K. S. Pedersen, and H. P. Ronningsen, "A Thermodynamic Model for Predicting Wax Formation in Crude Oils," *AIChE J.*, **34**(12), 1937 (1988).
Johnson, N. L., and S. Kotz, *Continuous Univariate Distributions: I*, Houghton Mifflin, Boston (1970).
Madsen, H. E. L., and R. Boistelle, "Solubility of Long-Chain *n*-Paraffins in Pentane and Heptane," *J. Chem. Soc., Faraday Trans.*, **72**, 1078 (1976).
Madsen, H. E. L., and R. Boistelle, "Solubility of Octacosane and Hexatriacontane in Different n-Alkane Solvents," *J. Chem. Soc., Farad. Trans.*, **75**, 1254 (1979).
Michelsen, M. L., "The Isothermal Flash Problem: I. Stability," *Fluid Phase Equil.*, **9**, 1 (1982).
Parks, G. S., G. E. Moore, M. L. Renquist, B. F. Naylor, L. A. McClaine, S. P. Fuji, and J. A. Hatton, "Thermal Data on Organic Compounds: XXV. Some Heat Capacity, Entropy and Free Energy Data for Nine Hydrocarbons of High Molecular Weight," *J. Phys. Chem.*, **71**, 3386 (1949).
Pedersen, W. B., A. B. Hansen, E. Larsen, A. B. Nielsen, and H. P. Ronningsen, "Wax Precipitation from North-Sea Crude Oils: 2. Solid-Phase Content as Function of Temperature Determined by Pulsed NMR," *Energy and Fuels*, **5**, 908 (1991).
Pedersen, K. S., P. Skovborg, and H. P. Ronningsen, "Wax Precipitation from North-Sea Crude Oils: 4. Thermodynamic Modeling," *Energy and Fuels*, **5**, 924 (1991).
Pedersen, K. S., "Prediction of Cloud-Point Temperatures and Amount of Wax Precipitation," paper SPE 27629, Soc. of Pet. Engrs., Richardson, TX (1993).
Peng, D.-Y., and D. B. Robinson, "A New Two-Constant Equation of State," *Ind. Eng. Chem. Fund.*, **15**, 59 (1976).
Prausnitz, J. M., R. N. Lichtenthaler, and E. G. Azevedo, *Molecular Thermodynamics of Fluid Phase Equilibria*, Chap. 9, Prentice-Hall, Englewood Cliffs, NJ (1986).
Riazi, M. R., and T. E. Daubert, "Simplify Property Predictions," *Hyd. Proc.*, 115 (Mar., 1980).
Robinson, D. B., D. Y. Peng, and S. Y.-K. Chung, "The Development of the Peng-Robinson Equation and Its Application to Phase Equilibrium in a System Containing Methanol," *Fluid Phase Equil.*, **24**, 25 (1985).
Ronningsen, H. P., B. Bjørndal, A. B. Hansen, and W. S. Pedersen, "Wax Precipitation from North Sea Crude Oils: I. Crystallization and Dissolution Temperature, and Newtonian and Non-Newtonian Flow Properties," *Energy & Fuel*, **5**, 895 (1991).
Snyder, R. G., M. C. Goh, V. J. P. Srivatsavoy, H. L. Strauss, and D. L. Dorset, "Measurement of the Growth Kinetics of Microdomains in Binary *n*-Alkane Solid Solutions by Infrared Spectroscopy," *J. Phys. Chem.*, **96**, 10008 (1992).
Snyder, R. G., G. Conti, H. L. Strauss, and D. L. Dorset, "Thermally-Induced Mixing in Partially Microphase Segregated Binary *n*-Alkane Crystals," *J. Phys. Chem.*, **97**, 7342 (1993).
Snyder, R. G., V. J. P. Srivatsavoy, D. A. Cates, H. L. Strauss, J. W. White, and D. L. Dorset, "Hydrogen/Deuterium Isotope Effects on Microphase Separation in Unstable Crystalline Mixtures of Binary *n*-Alkanes," *J. Phys. Chem.*, **98**, 674 (1994).
Soave, G., "Equilibrium Constants from a Modified Redlich-Kwong Equation of State," *Chem. Eng. Sci.*, **27**, 1197 (1972).
Spaght, M. E., S. B. Thomas, and G. S. Parks, "Some Heat-Capacity Data on Organic Compounds Obtained with a Radiation Calorimeter," *J. Phys. Chem.*, **36**, 882 (1932).
Twu, C. H., "An Internally Consistent Correlation for Predicting the Critical Properties and Molecular Weights of Petroleum and Coal-Tar Liquids," *Fluid Phase Equil.*, **16**, 137 (1984).
Whitson, C. H., "Characterizing Hydrocarbon Plus Fractions," *Soc. Pet. Eng. J.*, 683 (1983).
Won, K. W., "Thermodynamics for Solid Solution-Liquid-Vapor Equilibria: Wax Phase Formation from Heavy Hydrocarbon Mixtures," *Fluid Phase Equil.*, **30**, 265 (1986).
Won, K. W., "Thermodynamic Calculation of Cloud Point Temperatures and Wax Phase Compositions of Refined Hydrocarbon Mixtures," *Fluid Phase Equil.*, **53**, 377 (1989).

Appendix: Model Formulation

Consider a system of N_s precipitating species, and N components. The equations of phase equilibrium are

(1) N vapor–liquid isofugacity equations

$$f_i^v(P,T,y_1,y_2,\ldots,y_{N-1}) - f_i^l(P,T,x_1,x_2,\ldots,x_{N-1}) = 0 \qquad (i=1,\ldots,N). \quad \text{(A1)}$$

(2) N_S liquid–solid isofugacity equations

$$f_i^l(P,T,x_1,x_2,\ldots,x_{N-1}) - f^s_{\text{pure}\,i}(P,T) = 0 \qquad [i=(N-N_s)+1,\ldots,N]. \quad \text{(A2)}$$

(3) $N-1$ material–balance equations

(*a*) For the nonprecipitating components:

$$z_i - x_i^l\left[1 - \sum_j^{N_s} S_j/F - \frac{V}{F}\right] - K_i^{vl}x_i^l\frac{V}{F} = 0 \qquad [i=1,\ldots,(N-N_s)]. \quad \text{(A3)}$$

(*b*) For precipitating components, where all solid phases are pure:

$$z_i - x_i^l\left[1 - \sum_j^{N_s} S_j/F - \frac{V}{F}\right] - S_i/F - K_i^{vl}x_i^l\frac{V}{F} = 0 \qquad [i=(N-N_s)+1,\ldots,N-1] \quad (N_s>1) \quad \text{(A4)}$$

where $K_i^{vl} = \varphi_i^l(P,T,\mathbf{x}^l)/\varphi_i^v(P,T,\mathbf{y})$.

Manuscript received July 22, 1994, and revision received Feb. 3, 1995.